J. Phys. B: At. Mol. Opt. Phys. **42** (2009) 095101 (9pp) doi:10.1088/0953-4075/42/9/095101

Electron re-scattering from aligned linear molecules using the *R*-matrix method

A G Harvey and J Tennyson

Department of Physics and Astronomy, University College London, London WC1E 6BT, UK

E-mail: j.tennyson@ucl.ac.uk

Received 12 January 2009, in final form 13 March 2009
Published 21 April 2009
Online at stacks.iop.org/JPhysB/42/095101

Abstract

Electron re-scattering in a strong laser field provides an important probe of molecular structure and processes. The laser field drives the ionization of the molecule, followed by acceleration and subsequent recollision of the electron with the parent molecular ion, the scattered electrons carry information about the nuclear geometry and electronic states of the molecular ion. It is advantageous in strong field experiments to work with aligned molecules, which introduces extra physics compared to the standard gas-phase, electron–molecule scattering problem. The formalism for scattering from oriented linear molecules is presented and applied to H_2 and CO_2. Differential cross sections are presented for (re-)scattering by these systems concentrating on the most common, linear alignment. In H_2 these cross sections show significant angular structure which, particularly for a scattering angle of 90°, are predicted to vary significantly between re-collisions stimulated by an even or an odd number of photons. In CO_2 these cross sections are zero indicating the necessity of using non-parallel alignment with this molecule.

(Some figures in this article are in colour only in the electronic version)

1. Introduction

Electron re-scattering in conjunction with high harmonic generation can allow for time-resolved study of nuclear and electronic dynamics at subfemtosecond timescales with Ångstrom spatial resolution [1–5], see [6] for a general review of the attosecond physics area. In such experiments a molecule is ionized in a strong, few cycle, laser field. The changes in sign of the laser field during the cycle can cause the electron to re-collide with its parent molecular ion. Under these circumstances the electron can either recombine leading to high harmonic generation (HHG) or it can be re-scattered. This scattering can be thought of as electron self-diffraction and the process has the potential to act as a detailed probe of the target molecule [2]. It is usual for such experiments to be performed on aligned molecules which enhance the probability of re-collision.

It is important for the understanding and analysis of such experiments to have a physically sound theoretical model of re-scattering which is capable of treating quantum mechanically the complicated scattering dynamics of an electron–molecular ion collision. We are exploring the use of sophisticated *ab initio* quantum-mechanical techniques to model this part of the re-scattering process. Previous theoretical models of the re-collision problem have largely employed a greatly simplified treatment of the electron dynamics in the re-scattering step [1, 7, 8].

In our model re-scattering is treated as equivalent to electron scattering from the corresponding molecular cation with the equilibrium nuclear geometry of the neutral molecule, the molecular axis is aligned parallel to the laser field and hence to the incident electron trajectory. We do not include the effects of the laser field, with the intention of incorporating our field-free scattering amplitudes into a strong field model in the future. This work builds upon a preliminary model that did not include molecular alignment [9]. Both previously and here we focus on molecular hydrogen and carbon dioxide; two molecules well suited to experimental study (e.g. [10–12]). However the theoretical techniques being used are general and offer great flexibility, so can be applied to other small molecules of interest. We note that dipole selection rules and linearly polarised light means that for a closed shell, symmetric, linear molecule, such as H_2 or CO_2, aligned parallel to the laser field, the total collision symmetry must

be either $^1\Sigma_g^+$, which requires an even number of photons to be absorbed, or $^1\Sigma_u^+$, which requires an odd number. We therefore concentrate on these symmetries below.

In this work, we use the *R*-matrix method to investigate re-scattering. The UK molecular *R*-matrix codes [13] give a general implementation of the *R*-matrix method for low (and intermediate [14]) electron collision energies. It has been widely used to study electron collisions with a variety of molecular ions but had no facilities for aligning molecules. In this paper we describe the theoretical and computational methods required to add this functionality, and present results from simulations of re-scattering from H_2 and CO_2. Note that very recently Colgan *et al* have undertaken a similar development for the case of electron impact ionisation [15].

2. The *R*-matrix method

The *R*-matrix method is an *ab initio* and fully quantum-theoretical technique particularly well suited to electron scattering problems [16]. It divides the configuration space of the molecular target into an inner and outer region. In the inner region, the scattering electron interacts with the bound electrons through exchange and electron–electron correlation. Rigorous techniques from quantum chemistry are used to account for these interactions, giving wavefunctions independent of the incident electron energy. The outer region reduces to a potential scattering problem where a single electron moves in the long-range multi-pole potential of the molecule. Only the outer region problem needs to be solved as a function of electron energy. This is of particular importance for problems, such as those considered here, involving electron collisions with molecular ions since the strong energy dependence of these collisions means that calculations need to be repeated for a large number of energies to obtain reliable results.

The wavefunctions computed in the inner and outer regions are matched on the *R*-matrix boundary, the solution is then propagated outwards asymptotically to give *T* or *K* matrices, which are alternate forms of the scattering matrix *S*.

3. Theory

Both HHG and re-scattering are enhanced at certain molecular alignments. At present our procedure averages out the orientational dependence of the scattering amplitude. We need to extend the *R*-matrix code so as to allow the scattering amplitude to be calculated from a linear molecule of specified alignment. We describe the more complex case of $D_{\infty h}$ molecules, for $C_{\infty v}$ molecules we simply need to suppress the summation over gerade and ungerade symmetries, denoted ν below, and relax the parity restrictions on the initial and final electron angular momenta, denoted l_i and l_j respectively below.

We start from the multichannel stationary wavefunction, Ψ_I^+, describing scattering of an incident electron with kinetic energy $E_i = \frac{1}{2}k_i^2$ and spin projection m_{s_i} on the molecular axis from an N electron target molecule of electronic state ψ_i (note: both k_i and $\mathbf{r}$ are in the LAB frame). The subscripts i and I are short for the quantum numbers $\{\Lambda_i, S_i, M_{S_i}, \nu_i\}$ needed to specify the electronic state of the target molecule and the quantum numbers $\{\Lambda_i, S_i, M_{S_i}, \nu_i, m_{s_i}\}$ for the $N+1$ system, respectively,

$$\Psi_I^+(x_1', \ldots, x_N'\sigma'\mathbf{r}) = \psi_i(x_1', \ldots, x_N')\chi_{\frac{1}{2}m_{s_i}}(\sigma')\mathrm{e}^{\mathrm{i}\mathbf{k}_i\cdot\mathbf{r}} + \sum_J \psi_j(x_1', \ldots, x_N')\chi_{\frac{1}{2}m_{s_j}}(\sigma')F_{\mathbf{k}_i I\mathbf{k}_j J}(\alpha, \beta, \gamma)\mathrm{e}^{\mathrm{i}k_j r}/r. \tag{1}$$

Here Λ_i is the projection of the angular momentum on the molecular axis, S_i is the spin, M_{S_i} is the spin projection on the molecular axis, ν_i is the gerade/ungerade nature of the state and m_{s_i} is the spin projection of the incident electron. The Euler angles (α, β, γ) specify the orientation of the molecule. It will be useful later in our derivation to think in terms of the quantum numbers $\{\Lambda, S, M_S, \nu\}$ of the $N+1$ system of the target plus the scattering electron as these are invariant throughout the collision.

The standard relation between the scattering amplitude and the *T*-matrix with plane wave asymptotic boundary conditions is [17]

$$F_{\mathbf{k}_i I\mathbf{k}_j J}(\alpha, \beta, \gamma) = 2\pi\mathrm{i}T_{\mathbf{k}_i I\mathbf{k}_j J}(\alpha, \beta, \gamma). \tag{2}$$

The above equation looks very simple, but unfortunately the *T*-matrix is in the LAB frame with a momentum basis while our *R*-matrix software delivers MOL frame *T*-matrices in an angular momentum basis and uses the invariants of the system to simplify the calculations. Our task then is to find the transformation that relates the MOL frame *T*-matrices and the LAB frame *T*-matrices. In the following discussion, we take the LAB frame as our starting point, and make the necessary transformations to relate it to the MOL frame. First we transform from the spin uncoupled to the spin coupled representation

$$F_{IJ} = 2\pi\mathrm{i}\sum_{S'M_S'SM_S}\left\langle S_j M_{S_j}\frac{1}{2}m_{s_j}\middle|S'M_S'\right\rangle T^S_{\mathbf{k}_i\bar{i}\mathbf{k}_j\bar{j}} \times \left\langle SM_S\middle|S_i M_{S_i}\frac{1}{2}m_{s_i}\right\rangle, \tag{3}$$

note that M_{S_i} and m_{s_i} are now undetermined so I becomes $\bar{i} = \{\Lambda_i, S_i, \nu_i\}$, also the *T*-matrix does not depend on M_S. The sum over S, S', M_S and M_S' becomes a sum over S and M_S as they are invariant in the $N+1$ system. Also putting $C_i = \langle SM_S|S_i M_{S_i}\frac{1}{2}m_{s_i}\rangle$ we get

$$F_{IJ} = 2\pi\mathrm{i}\sum_{SM_S} C_j T^S_{\mathbf{k}_i\bar{i}\mathbf{k}_j\bar{j}} C_i. \tag{4}$$

The next step is to transform from plane wave to angular momentum asymptotic states, this is a partial wave expansion. To aid in this we need the transformation equation [17]

$$\langle E_i l_i m_{l_i}|\mathbf{k}_i\rangle = \frac{\mathrm{i}^{l_i}}{\sqrt{k_i}}Y_{l_i}^{m_{l_i}*}(\hat{k}_i), \tag{5}$$

this gives

$$F_{IJ} = 2\pi\mathrm{i}\frac{1}{\sqrt{k_i k_j}} \times \sum_{\substack{SM_S \\ l_i l_j m_{l_i}' m_{l_j}'}} \mathrm{i}^{l_i - l_j}Y_{l_j}^{m_{l_j}'}(\hat{k}_j)C_j T^S_{\bar{i}l_i m_{l_i}\bar{j}l_j m_{l_j}} C_i^* Y_{l_i}^{m_{l_i}'*}(\hat{k}_i'), \tag{6}$$

where l_i is the angular momentum quantum number of the scattering electron and m'_{l_i} is its projection onto the z'-axis (here the prime indicates the MOL frame). Now to express the LAB frame T-matrix in terms of the molecular frame T-matrix, where R is the rotation operator, specified by the Euler angles (α, β, γ), representing a rotation from the MOL to the LAB frame,

$$T_{\mathrm{LAB}} = RT_{\mathrm{MOL}}R^{\dagger} \tag{7}$$

$$= \sum_{m'_{l_j} m'_{l_i}} \left\langle E_j l_j m_{l_j} \middle| R \middle| E_j l_j m'_{l_j} \right\rangle T_{\mathrm{MOL}} \left\langle E_i l_i m'_{l_i} \middle| R^{\dagger} \middle| E_i l_i m_{l_i} \right\rangle \tag{8}$$

$$= \sum_{m'_{l_j} m'_{l_i}} D^{l_j}_{m_{l_j} m'_{l_j}}(\alpha, \beta, \gamma) T_{\mathrm{MOL}} D^{l_i *}_{m_{l_i} m'_{l_i}}(\alpha, \beta, \gamma), \tag{9}$$

here the Wigner D-matrix elements, $D^{l_i *}_{m_{l_i} m'_{l_i}}(\alpha, \beta, \gamma)$, relate the angular momentum states in the two frames [18]. With equation (6) this gives

$$F_{IJ} = \frac{2\pi \mathrm{i}}{\sqrt{k_i k_j}} \sum_{\substack{\Lambda S M_S \nu \\ l_i l_j m_{l_i} m_{l_j} m'_{l_i} m'_{l_j}}} \mathrm{i}^{l_i - l_j} D^{l_j}_{m_{l_j} m'_{l_j}} Y^{m_{l_j}}_{l_j}(\hat{k}_j) C_j \times T^{S}_{\bar{l}_i m_{l_i} \bar{j} l_j m_{l_j}} C_i^* D^{l_i *}_{m_{l_i} m'_{l_i}} Y^{m_{l_i} *}_{l_i}(\hat{k}_i). \tag{10}$$

Now we change our summation over m'_{l_i} into a summation over the conserved quantity Λ, by recognizing that $m'_{l_i} = \Lambda - \Lambda_i$ and that Λ_i is fixed. We can see that the Λ invariance implies m'_{l_i} and m'_{l_j} are not independent of each other, in fact $m'_{l_j} = m'_{l_i} + (\Lambda_i - \Lambda_j)$. Also the preceding relation and the value of Λ gives a lower limit to the possible values of l_i and l_j. Finally we should note that Λ, Λ_i and Λ_j can take positive, zero and negative values, of course positive and negative states with the same value are degenerate due to the cylindrical symmetry of the system. It is also convenient to introduce a sum over the invariant ν which will restrict our l_i values in the following manner. $\bar{l}_i$ runs over values satisfying $(-1)^{\bar{l}_i} \nu_i = \nu$. Giving

$$F_{IJ} = \frac{2\pi \mathrm{i}}{\sqrt{k_i k_j}} \sum_{\substack{\Lambda S M_S \nu \\ \bar{l}_i \bar{l}_j m_{\bar{l}_i} m_{\bar{l}_j}}} i^{\bar{l}_i - \bar{l}_j} D^{\bar{l}_j}_{m_{\bar{l}_j} \Lambda - \Lambda_j} Y^{m_{\bar{l}_j}}_{\bar{l}_j}(\hat{k}_j) C_j \times T^{\Lambda S \nu}_{\bar{i} \bar{l}_i \bar{j} \bar{l}_j} C_i^* D^{\bar{l}_i *}_{m_{\bar{l}_i} \Lambda - \Lambda_i} Y^{m_{\bar{l}_i} *}_{\bar{l}_i}(\hat{k}_i), \tag{11}$$

which we can simplify further by setting our LAB frame z-axis to lie along the incident electron direction. From the properties of spherical harmonics we get

$$Y^{m_{\bar{l}_i} *}_{\bar{l}_i}(0, \phi_i) = \frac{\sqrt{2\bar{l}_i + 1}}{\sqrt{4\pi}} \delta_{m_{\bar{l}_i} 0}, \tag{12}$$

substituting this into the transformation equation for the spherical harmonics we get

$$\sum_{m_{\bar{l}_i}} D^{\bar{l}_i}_{m_{\bar{l}_i} \Lambda - \Lambda_i} Y^{m_{\bar{l}_i}}_{\bar{l}_i}(0, \phi_i) = D^{\bar{l}_i}_{0 \Lambda - \Lambda_i} \frac{\sqrt{2\bar{l}_i + 1}}{\sqrt{4\pi}}, \tag{13}$$

giving

$$F_{IJ} = \frac{\sqrt{\pi} \mathrm{i}}{\sqrt{k_i k_j}} \sum_{\substack{\Lambda S M_S \nu \\ \bar{l}_i \bar{l}_j m_{\bar{l}_j}}} i^{\bar{l}_i - \bar{l}_j} \times \sqrt{2\bar{l}_i + 1} D^{\bar{l}_j}_{m_{\bar{l}_j} \Lambda - \Lambda_j} Y^{m_{\bar{l}_j}}_{\bar{l}_j}(\hat{k}_j) C_j T^{\Lambda S \nu}_{\bar{i} \bar{l}_i \bar{j} \bar{l}_j} C_i^* D^{\bar{l}_i *}_{0 \Lambda - \Lambda_i} \tag{14}$$

which is the same as equation (5) given by Malegat [19], although our derivation differs. To get the differential cross section from the scattering amplitude we use

$$\frac{\mathrm{d}\sigma}{\mathrm{d}\Omega} = \frac{k_j}{k_i} |F_{IJ}|^2, \tag{15}$$

which gives us

$$\frac{\mathrm{d}\sigma}{\mathrm{d}\Omega} = \frac{\pi}{k_i^2} \sum_{\substack{\Lambda S M_S \nu \\ \Lambda' S' M'_S \nu'}} \sum_{\substack{\bar{l}_i \bar{l}_j m_{\bar{l}_j} \\ \bar{l}'_i \bar{l}'_j m'_{\bar{l}_j}}} \mathrm{i}^{\bar{l}_i - \bar{l}_j - \bar{l}'_i + \bar{l}'_j} \times \sqrt{(2\bar{l}_i + 1) 2\bar{l}'_i + 1)} C_i C_j C'_i C'_j \times D^{\bar{l}_j}_{m_{\bar{l}_j} \Lambda - \Lambda_j} D^{\bar{l}'_j *}_{m'_{\bar{l}_j} \Lambda' - \Lambda_j} D^{\bar{l}_i *}_{0 \Lambda - \Lambda_i} D^{\bar{l}'_i *}_{0 \Lambda' - \Lambda_i} \times Y^{m_{\bar{l}_j}}_{\bar{l}_j} Y^{m'_{\bar{l}_j} *}_{\bar{l}'_j} T^{\Lambda S \nu}_{\bar{i} \bar{l}_i \bar{j} \bar{l}_j} T^{\Lambda' S' \nu' *}_{\bar{i} \bar{l}'_i \bar{j} \bar{l}'_j}. \tag{16}$$

We assume that the spin polarization of the scattering electron, and of the target are not measured. This implies that as the initial spin states are unknown we must average over them. Also because the final states are not measured we do not distinguish between differential cross sections from different spin polarizations and hence must sum over them as is standard in scattering theory. Performing the summation we get

$$\frac{\mathrm{d}\sigma}{\mathrm{d}\Omega} = \frac{\pi}{k_i^2 2(2S_i + 1)} \sum_S (2S + 1) \sum_{\substack{\Lambda \nu \\ \Lambda' \nu'}} \sum_{\substack{\bar{l}_i \bar{l}_j m_{\bar{l}_j} \\ \bar{l}'_i \bar{l}'_j m'_{\bar{l}_j}}} \mathrm{i}^{\bar{l}_i - \bar{l}_j - \bar{l}'_i + \bar{l}'_j} \times \sqrt{(2\bar{l}_i + 1) 2\bar{l}'_i + 1)} D^{\bar{l}_j}_{m_{\bar{l}_j} \Lambda - \Lambda_j} D^{\bar{l}'_j *}_{m'_{\bar{l}_j} \Lambda' - \Lambda_j} \times D^{\bar{l}_i *}_{0 \Lambda - \Lambda_i} D^{\bar{l}'_i *}_{0 \Lambda' - \Lambda_i} Y^{m_{\bar{l}_j}}_{\bar{l}_j} Y^{m'_{\bar{l}_j} *}_{\bar{l}'_j} T^{\Lambda S \nu}_{\bar{i} \bar{l}_i \bar{j} \bar{l}_j} T^{\Lambda' S \nu' *}_{\bar{i} \bar{l}'_i \bar{j} \bar{l}'_j}, \tag{17}$$

after contraction of the rotation matrix elements and also of the spherical harmonics we get

$$\frac{\mathrm{d}\sigma}{\mathrm{d}\Omega} = \frac{\pi^{\frac{1}{2}} (-1)^{\Lambda_i + \Lambda_j}}{4(2S_i + 1) k_i^2} \sum_{\substack{\Lambda \nu \bar{l}_i \bar{l}_j \\ \Lambda' \nu' \bar{l}'_i \bar{l}'_j}} \sum_{L_i K} \mathrm{i}^{\bar{l}_i - \bar{l}_j - \bar{l}'_i + \bar{l}'_j} \times \sqrt{(2\bar{l}_i + 1) 2\bar{l}'_i + 1) 2\bar{l}_j + 1) 2\bar{l}'_j + 1)} \times \langle \bar{l}_i 0 \bar{l}'_i 0 | L_i 0 \rangle \langle \bar{l}_j 0 \bar{l}'_j 0 | K 0 \rangle \times \langle \bar{l}_i \Lambda - \Lambda_i \bar{l}'_i \Lambda_i - \Lambda' | L_i \Lambda - \Lambda' \rangle \times \langle \bar{l}_j \Lambda - \Lambda_j \bar{l}'_j \Lambda_j - \Lambda' | K \Lambda - \Lambda' \rangle \times D^{K}_{m_{\bar{l}_j} - m'_{\bar{l}_j}, \Lambda - \Lambda'} D^{L_i}_{0, \Lambda - \Lambda'} \times \sum_S (2S + 1) T^{\Lambda S \nu}_{\bar{i} \bar{l}_i \bar{j} \bar{l}_j} T^{\Lambda' S \nu'}_{\bar{i} \bar{l}'_i \bar{j} \bar{l}'_j} Y^{m_{l_j} - m_{l_{j'}}}_{K}(\hat{k}_j). \tag{18}$$

Finally, we note that if the sign of Λ_i and Λ_j is not measured we must average the differential cross section given above over the degenerate initial target states and sum over the degenerate final target states.

We have written a program to implement the above formalism that calculates scattering amplitudes, differential and integral cross sections from aligned linear molecules.

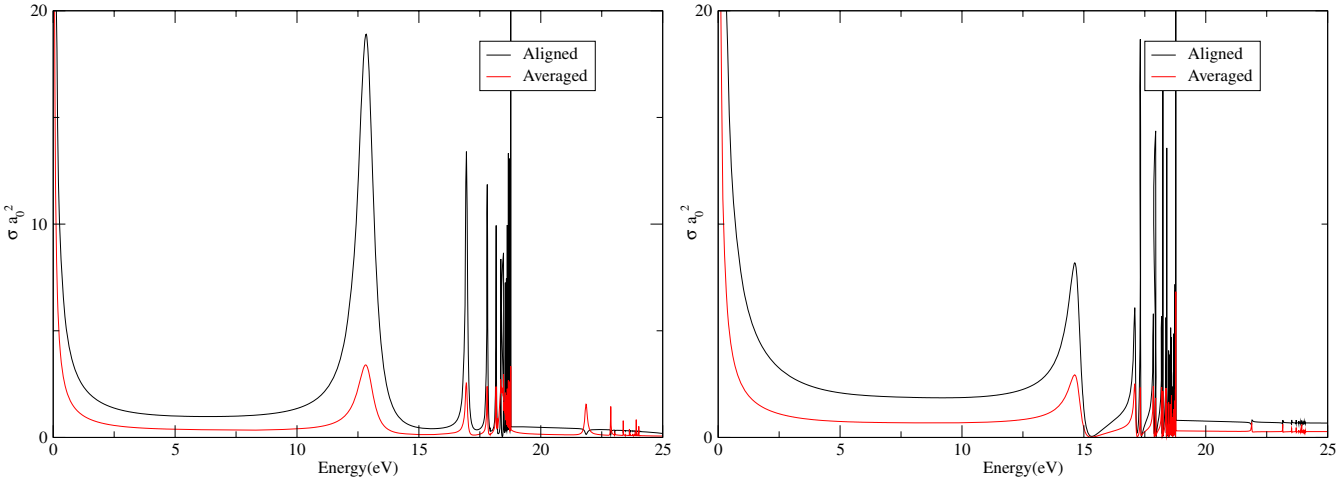

Figure 1. Total cross section as a function of energy for the parallel aligned electron—H_2^+ collision problem: left figure: $^1\Sigma_g^+$ total symmetry, right figure: $^1\Sigma_u^+$ symmetry.

For polyatomic molecules there is one further technical issue that needs to be addressed. The above formalism is sufficient for calculations on diatomic systems for which the UK molecular *R*-matrix method uses full linear molecule symmetry [13]. However the polyatomic version of the code only uses Abelian point groups, this means that calculations on symmetric or asymmetric linear molecules are performed using the D_{2h} or C_{2v} point groups, respectively. Application of the above formalism requires the reconstruction of *T*-matrices into the linear molecule symmetry groups $D_{\infty h}$ or $C_{\infty v}$ [20]. Details of how to do this are given in the appendix.

4. Results

4.1. Molecular hydrogen

H_2 is a homonuclear diatomic and a member of the $D_{\infty h}$ point group. In our calculation we consider a rigid molecule with the internuclear separation frozen at 1.4 a_0. The molecular axis is aligned parallel to the incident electron direction. The close-coupling expansion includes the lowest three states of the H_2^+ target ion which are of $^2\Sigma_g^+$, $^2\Sigma_u^+$ and $^2\Pi_u$ symmetry.

Figure 1 shows the total cross section for electron re-scattering from parallel aligned H_2 against incident electron energy. The cross sections are approximately 3–4 times greater in magnitude than the orientationally averaged case, this is what we might expect taking the simplistic view that the electron takes a longer path through the molecule and so has more opportunity to interact with it. Compared to previous, orientationally averaged calculations [9, 21], they show similar resonance structure up to the first electronic excitation threshold; however, the series of Feshbach resonances converging on the second excited state are heavily suppressed.

Figure 2 shows parallel aligned differential cross sections for a range of non-resonant energies. With this alignment, due to the symmetry of the system, the differential cross section is a function of θ, the polar angle, alone. We see that $^1\Sigma_g^+$ symmetry differential cross sections are markedly different in shape than the orientationally averaged case. All the differential cross sections are symmetric about 90°; this is to be expected as elastic scattering of single total symmetry will have a continuum described entirely by a sum of either gerade or ungerade spherical harmonics depending on the gerade/ungerade symmetry of the target state; these sums are symmetric around 90°. For energies below the first resonance at 12.87 eV, we can see that the differential cross sections have strong peaks in the forwards and backwards directions and slightly lower peaks at 90°. Interestingly at 15.5 eV, in between the first and second resonances, we see a significant change in shape that appears to be an inversion, with minima in the forwards and backwards directions. This may be a phase effect due to passing through the first resonance. Above the first excited state we again get strong forwards and backwards scattering, however the peak at 90° is significantly less pronounced. The $^1\Sigma_u^+$ symmetry shows strong forwards and backwards scattering, unlike $^1\Sigma_g^+$ symmetry, there is no sideways scattering and no significant shape difference between the aligned and orientationally averaged cases, or change of shape as a function of energy.

In figure 3, we have plotted total cross section versus alignment angle β. We see that both the $^1\Sigma_g^+$ and $^1\Sigma_u^+$ components are strongly peaked for parallel alignment, with $^1\Sigma_g^+$ having an additional smaller peak at perpendicular alignment while $^1\Sigma_u^+$ is zero. Due to the $^2\Sigma_g^+$ ground state of the cation we expect the contribution of higher symmetries for non-parallel alignments to be relatively minor. These observations justify the use of parallel alignment in re-scattering experiments on H_2.

4.2. Carbon dioxide

CO_2 is a linear triatomic molecule and is also a member of the $D_{\infty h}$ point group. In our calculation the two CO bondlengths were frozen at their equilibrium value of 2.196 a_0 [22]. The coupled-states expansion includes the lowest four

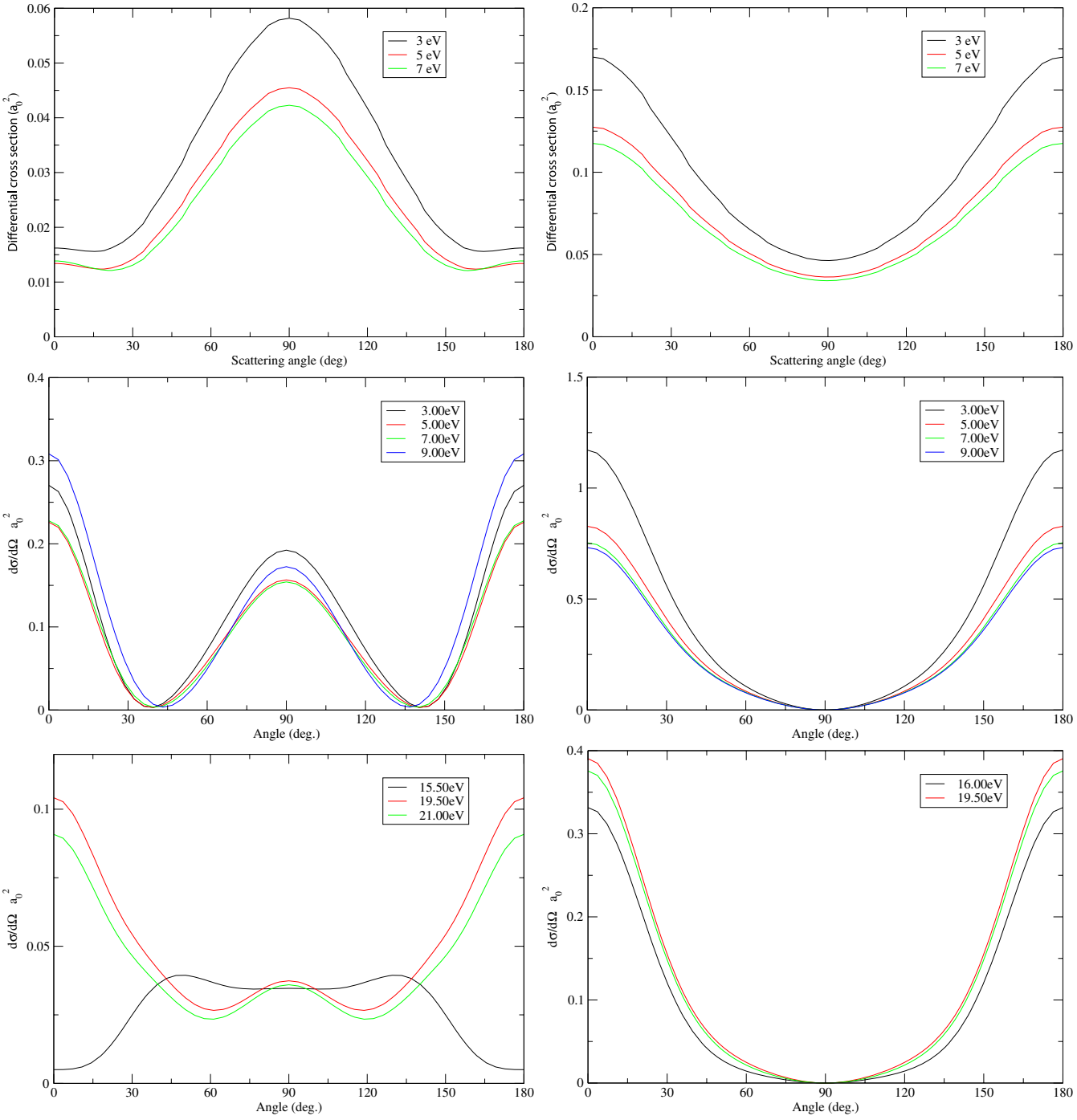

Figure 2. Differential cross sections for parallel aligned electron–H_2^+ collisions for seven electron collision energies (top row: orientationally averaged case): left-hand figures: $^1\Sigma_g^+$ symmetry, right-hand figures: $^1\Sigma_u^+$ symmetry.

states of the CO_2^+ target ion which have $^2\Pi_g$, $^2\Pi_u$, $^2\Sigma_u^+$ and $^2\Sigma_g^+$ symmetries, respectively. As CO_2 has the same symmetry as H_2, the same dipole allowed selection rules apply for absorption of linearly polarized light by an oriented molecule. However the $^2\Pi_g$ symmetry of the cationic ground state introduces some significant differences from the hydrogenic case.

Our scattering calculation was performed using the UK *R*-matrix polyatomic code [13, 23] which only works in Abelian point groups. It was therefore necessary to transform our *T*-matrices from D_{2h} to $D_{\infty h}$ symmetry groups using a new module TMATMAP. This procedure is described in the appendix.

Figure 4 compares the orientationally averaged $D_{\infty h}$ total cross sections for $^1\Sigma_g^+$ and $^1\Sigma_u^+$ symmetries with the corresponding results for ^1A_g and $^1B_{1u}$ from our original D_{2h} calculations. As discussed in the appendix these are the D_{2h} symmetries which contain the $^1\Sigma^+$ contributions. We see that the ^1A_g and $^1B_{1u}$ D_{2h} symmetry cross sections are approximately 3–4 times larger than their respective $D_{\infty h}$

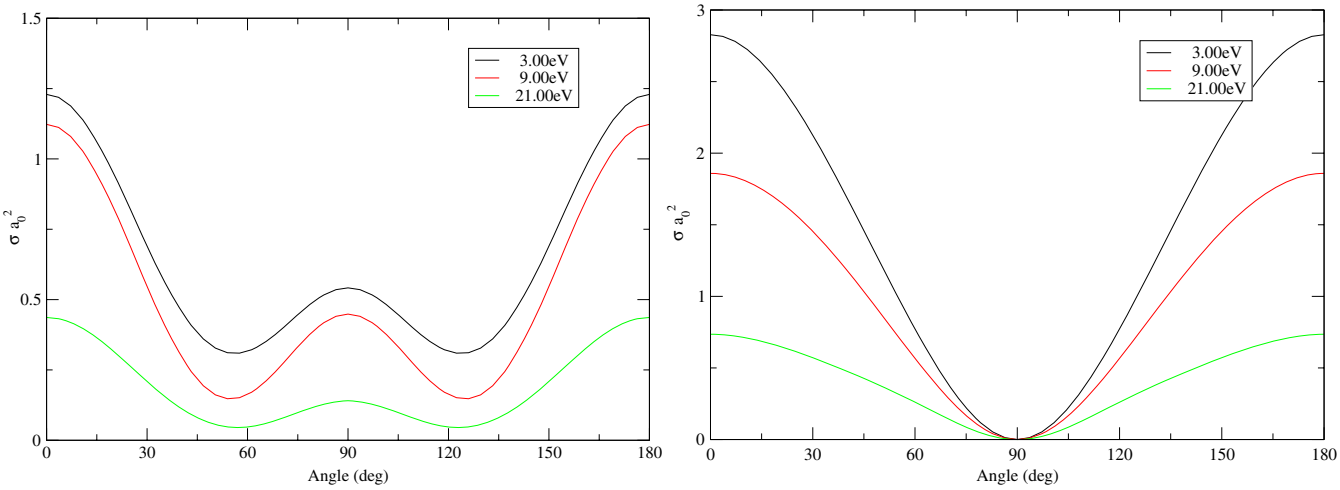

Figure 3. Total cross section as a function of alignment angle β for the aligned electron–H_2^+ collision problem at a range of energies—left figure: $^1\Sigma_g^+$ total symmetry, right figure: $^1\Sigma_u^+$ symmetry.

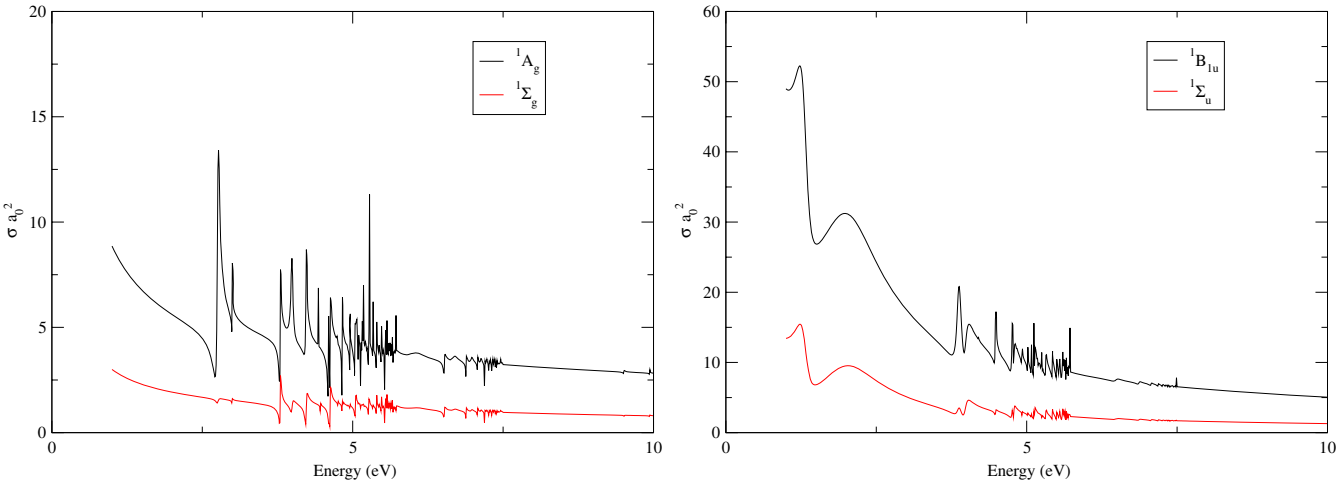

Figure 4. Total cross section as a function of energy for the orientationally averaged electron–CO_2^+ collision problem comparing original D_{2h} and transformed using TMATMAP $D_{\infty h}$ symmetries—left figure: ^1A_g and $^1\Sigma_g^+$ total symmetries, right figure: $^1B_{1u}$ and $^1\Sigma_u^+$ symmetries.

symmetry counterparts, $^1\Sigma_g^+$ and $^1\Sigma_u^+$. This is because the D_{2h} cross sections contain significant contributions from the $^1\Delta$ components. The $^2\Pi_g$ target and π continuum couple to give $^1\Sigma$ and $^1\Delta$ total symmetry and both these symmetries are contained in the corresponding D_{2h} T-matrix elements. It can be anticipated that cross sections of $^1\Pi_g$ total symmetry will be dominant at low collision energies as they couple to a σ_g continuum. We note that the resonance structure is unchanged, we still see infinite series of Feshbach resonances below each threshold [9], a higher energy resolution would resolve more of these.

Figure 5 shows total cross section for $^1\Sigma^+$ symmetries as a function of the alignment angle β. We immediately see that for both symmetries we get zero total cross section for the parallel aligned case and therefore zero differential cross sections; this is a direct consequence of the $^2\Pi_g$ symmetry of the CO_2^+ target. It is important to note that, for alignments other than parallel, it is necessary to sum over higher symmetries to give the correct differential cross sections, we expect these to be significant due to the $^2\Pi_g$ ground state of the cation. We see that for the $^1\Sigma_g^+$ component the cross sections have a maxima between 50–55° and 125–130° depending on energy and are zero at 90° and 0°.

For $^1\Sigma_u^+$ there is a maximum at 90° in contrast with $^1\Sigma_g^+$, and there are smaller peaks between 35–40° and 125–130°. These observations agree with the recent study on HHG with CO_2 by Mairesse *et al* [11].

Figure 6 shows the $^1\Sigma^+$ part of the differential cross section given in polar coordinates with r being the magnitude of the differential cross section. The differential cross sections are symmetrical around the molecular axis, this suggests that the z–x plane, containing the molecule, is an appropriate plane in which to examine them. We see that for $^1\Sigma_g^+$ the differential cross section is zero parallel and perpendicular to the molecular axis. $^1\Sigma_u^+$ is also zero in the parallel direction but has a small peak perpendicular to the molecular axis and is approximately 4 times greater in magnitude than $^1\Sigma_g^+$.

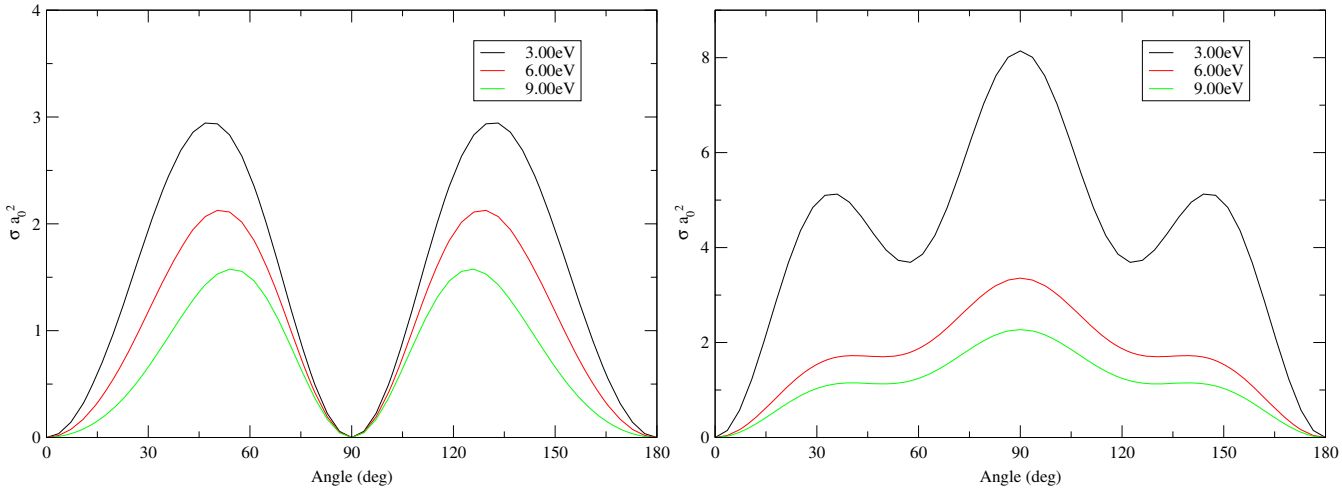

Figure 5. Total cross section as a function of alignment angle β for the aligned electron–CO_2^+ collision problem at a range of energies—left figure: $^1\Sigma_g^+$ total symmetry, right figure: $^1\Sigma_u^+$ symmetry.

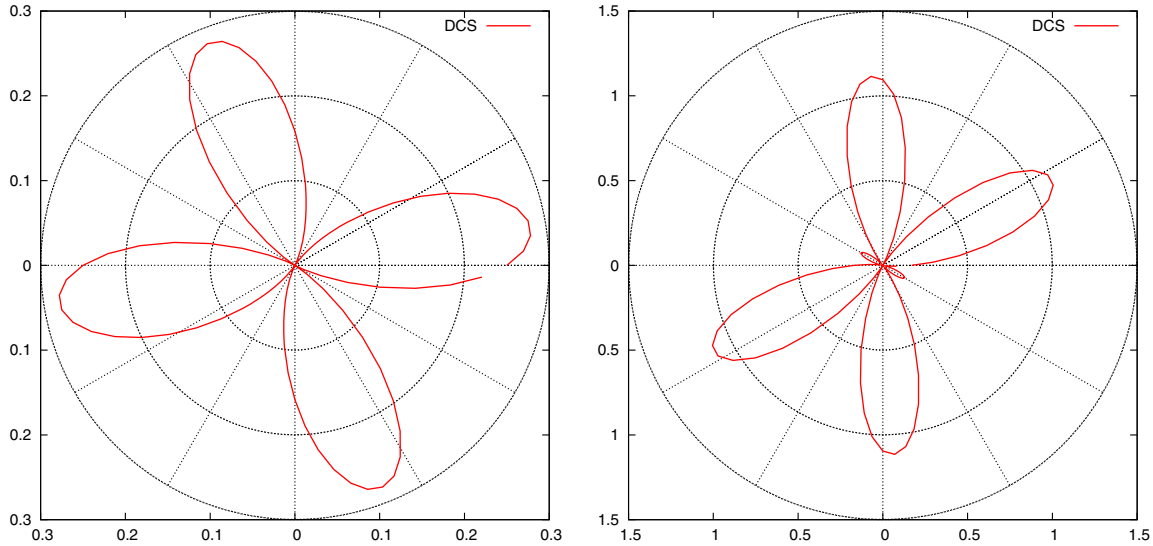

Figure 6. Polar plots of the differential cross section taken in the z–x plane with $\beta = 30^\circ$ for the aligned electron—CO_2^+ collision problem at 3 eV: left figure, $^1\Sigma_g^+$ total symmetry; right figure, $^1\Sigma_u^+$ symmetry. The scale is in units of a_0 and gives the r values for the circular grid.

5. Conclusions

We have developed analytic and computational methods for studying electron scattering from aligned molecules and present integral and differential cross sections for re-scattering from parallel aligned H_2 and CO_2. Our results for H_2 show that for the $^1\Sigma_g^+$ symmetry both integral and differential cross sections are greater in magnitude and that differential cross sections also differ in shape in comparison to the non-aligned situation. We see strong forwards and backwards scattering in contrast to the minima at these directions in the unaligned case. We also see that the shape of the differential cross section can change significantly before and after a resonance. $^1\Sigma_u^+$ differential cross sections showed a difference in magnitude but not shape in comparison to the unaligned case.

For CO_2 we find that parallel alignment gives zero cross sections indicating a need to perform this type of experiment at non-parallel alignments. We also see that perpendicular alignment gives a zero cross section for $^1\Sigma_g^+$ and a maximum for $^1\Sigma_u^+$ however further work to include higher symmetries is required to gain an accurate picture of non-parallel alignments.

We note that the latest models of re-collision find it important to explicitly allow for electron impact electronic excitation of the target ion [24]; this process is automatically included in our scattering treatment.

So far our studies have ignored the undeniably important effect of the external laser field on the scattering electron. It is straightforward to add a weak field using our current techniques [25] but adding a strong field requires a time-dependent treatment. There are two possible approaches to overcoming the omission of the laser field. One is to incorporate our scattering amplitudes into a strong field model. A second approach is to incorporate the laser effects within the R-matrix approach. We note that the formalism for this was given sometime ago [26] but has only recently been

implemented for the atomic case [27]. Generalization of this to molecular systems would give a consistent treatment of the problem but remains both technically and computationally challenging.

Acknowledgments

This work was performed as part of an EPSRC funded project to study ultra-fast molecular imaging. We acknowledge helpful discussions with all members of the consortium and in particular Jon Marangos, Misha Ivanov and Jonathan Underwood.

Appendix

We need to transform T-matrix elements calculated in D_{2h} symmetry into $D_{\infty h}$ symmetry when $D_{\infty h}$ is the natural symmetry of the system. Scattering channels are defined by target wavefunctions and continuum wavefunctions in the following manner. $\left|\psi_t^{\Lambda} Y_l^{\lambda}\right\rangle$ in $D_{\infty h}$ and $\left|\psi_t^{\Gamma} S_l^{\gamma}\right\rangle$ in D_{2h}, where Y_l^{λ} are the complex spherical harmonics and S_l^{γ} are the real spherical harmonics.

We know how to transform between complex and real spherical harmonics and so know how the continuum wavefunctions transform, we have

$$\begin{pmatrix} Y_l^m \\ Y_l^{-m} \end{pmatrix} = \frac{1}{\sqrt{2}} \begin{pmatrix} (-1)^m & (-1)^m \mathrm{i} \\ 1 & -\mathrm{i} \end{pmatrix} \begin{pmatrix} S_l^m \\ S_l^{-m} \end{pmatrix} m > 0 \qquad (A.1)$$

and

$$Y_l^0 = S_l^0. \qquad (A.2)$$

The transformation is straightforward for Σ symmetries as there is a one-to-one mapping between the $D_{\infty h}$ irreducible representations (IRs) Σ_g^+, Σ_u^+, Σ_g^-, Σ_u^- and the D_{2h} IRs A_g, B_{1u}, B_{1g}, A_u.

The target wavefunctions are more problematic. Formally they consist of linear combinations of products of N spherical harmonics, where N is the number of target molecule electrons. The problem is that although $\psi_t^{\Lambda} \epsilon \Gamma^1 \oplus \Gamma^2$, so are an infinite number of other IRs of $D_{\infty h}$. This means we cannot set up an isomorphism between IRs of $D_{\infty h}$ and the direct sum of IRs of D_{2h}. To proceed we need to make the following assumption.

It is always possible to associate the quantum number Λ with the direct sum of the relevant target states calculated under D_{2h}.

The justification for this is that the natural symmetry of the target molecule is $D_{\infty h}$ and the Hamiltonian implicitly has this symmetry hence any contamination of the D_{2h} target wavefunctions by other IRs of $D_{\infty h}$ is due to numerical error. This allows us to set up an isomorphism between $D_{\infty h}$ and D_{2h} decomposed as $(\Gamma^1 \oplus \Gamma^2)_{\Lambda}$.

For Σ target states we have a one-to-one mapping to the D_{2h} IRs A_g, B_{1u}, B_{1g}, A_u. For other symmetries one needs to know how the product space relates to the single spherical harmonic basis for non-sigma functions.

As l is not a good quantum number for $D_{\infty h}$ systems it is convenient to introduce the equivalence relation $Y_{l_1}^{m_1} \sim Y_{l_2}^{m_2}$ if $m_1 = m_2$, and l_1 and l_2 have the same parity. This gives us a set of equivalence classes $\left\{\left[Y_g^m\right], \left[Y_u^m\right]\right\}$. We can do the same for the real spherical harmonics and the transformation between the two remain the same if we replace the spherical harmonics with the equivalence classes. We can now set up an isomorphism between these equivalence classes and the irreducible representations in $D_{\infty h}$ and D_{2h}. This allows us to write

$$\begin{pmatrix} \psi_\nu^{\Lambda} \\ \psi_\nu^{-\Lambda} \end{pmatrix} \cong \begin{pmatrix} \left[Y_\nu^{\Lambda}\right] \\ \left[Y_\nu^{-\Lambda}\right] \end{pmatrix} = \frac{1}{\sqrt{2}} \begin{pmatrix} (-1)^{\Lambda} & (-1)^{\Lambda}\mathrm{i} \\ 1 & -\mathrm{i} \end{pmatrix} \begin{pmatrix} \left[S_\nu^{\Lambda}\right] \\ \left[S_\nu^{-\Lambda}\right] \end{pmatrix} \cong \begin{pmatrix} (-1)^{\Lambda} & (-1)^{\Lambda}\mathrm{i} \\ 1 & -\mathrm{i} \end{pmatrix} \begin{pmatrix} \psi_\nu^{\Gamma^1} \\ \psi_\nu^{-\Gamma^2} \end{pmatrix}_{\Lambda}. \qquad (A.3)$$

The $D_{\infty h}$ T-matrix elements can now be constructed from the relevant D_{2h} T-matrix elements. We have

$$\langle \Lambda_j \lambda_j | T | \Lambda_i \lambda_i \rangle = \left\langle \Gamma_j^1 \oplus \Gamma_j^2, \gamma_j^1 \oplus \gamma_j^1 \middle| T \middle| \Gamma_i^1 \oplus \Gamma_i^2, \gamma_i^1 \oplus \gamma_i^1 \right\rangle, \qquad (A.4)$$

using the transformation matrix and denoting its matrix elements $A_{pq}^{\Lambda_i}$ we get

$$\begin{aligned} \langle \Lambda_j \lambda_j | T | \Lambda_i \lambda_i \rangle = {} & A_{m1}^{\Lambda_j *} A_{n1}^{\lambda_j *} A_{r1}^{\Lambda_j} A_{s1}^{\lambda_j} \left\langle \Gamma_j^1 \gamma_j^1 \middle| T \middle| \Gamma_i^1 \gamma_i^1 \right\rangle \\ & + A_{m1}^{\Lambda_j *} A_{n1}^{\lambda_j *} A_{r2}^{\Lambda_j} A_{s2}^{\lambda_j} \left\langle \Gamma_j^1 \gamma_j^1 \middle| T \middle| \Gamma_i^2 \gamma_i^2 \right\rangle \\ & + A_{m2}^{\Lambda_j *} A_{n2}^{\lambda_j *} A_{r1}^{\Lambda_j} A_{s1}^{\lambda_j} \left\langle \Gamma_j^2 \gamma_j^2 \middle| T \middle| \Gamma_i^1 \gamma_i^1 \right\rangle \\ & + A_{m2}^{\Lambda_j *} A_{n2}^{\lambda_j *} A_{r2}^{\Lambda_j} A_{s2}^{\lambda_j} \left\langle \Gamma_j^2 \gamma_j^2 \middle| T \middle| \Gamma_i^2 \gamma_i^2 \right\rangle \\ & + A_{m1}^{\Lambda_j *} A_{n2}^{\lambda_j *} A_{r1}^{\Lambda_j} A_{s2}^{\lambda_j} \left\langle \Gamma_j^1 \gamma_j^2 \middle| T \middle| \Gamma_i^1 \gamma_i^2 \right\rangle \\ & + A_{m1}^{\Lambda_j *} A_{n2}^{\lambda_j *} A_{r2}^{\Lambda_j} A_{s1}^{\lambda_j} \left\langle \Gamma_j^1 \gamma_j^2 \middle| T \middle| \Gamma_i^2 \gamma_i^1 \right\rangle \\ & + A_{m2}^{\Lambda_j *} A_{n1}^{\lambda_j *} A_{r1}^{\Lambda_j} A_{s2}^{\lambda_j} \left\langle \Gamma_j^2 \gamma_j^1 \middle| T \middle| \Gamma_i^1 \gamma_i^2 \right\rangle \\ & + A_{m2}^{\Lambda_j *} A_{n1}^{\lambda_j *} A_{r2}^{\Lambda_j} A_{s1}^{\lambda_j} \left\langle \Gamma_j^2 \gamma_j^1 \middle| T \middle| \Gamma_i^2 \gamma_i^1 \right\rangle, \end{aligned} \qquad (A.5)$$

where the index m, n, r or s is 1 when the respective quantum number Λ_j, λ_j, Λ_i or λ_i is positive and 2 if negative. The first four terms in the summation are of total symmetry Γ_1, the second four are of symmetry Γ_2. The above expression is for the most complex case of degenerate initial target and continuum to degenerate final target and continuum, with degenerate total symmetry. For non-degenerate states one can replace the relevant coefficients with unity and reduce the number of elements summed over accordingly. For Σ total symmetry we find that the sum reduces to (up to) four elements, either the first four (Σ^+) or the last four (Σ^-). The above method was implemented in our code TMATMAP.

References

[1] Lein M, Marangos J P and Knight P L 2002 Electron diffraction in above-threshold ionization of molecules *Phys. Rev.* A **66** 051404

[2] Spanner M, Smirnova O, Corkum P B and Ivanov M Yu 2004 Reading diffraction images in strong field ionization of diatomic molecules *J. Phys. B: At. Mol. Opt. Phys.* **37** L243–L250

[3] Zuo T, Brandrauk A D and Corkum P B 1996 Laser-induced electron diffraction: a new tool for probing ultrafast molecular dynamics *Chem. Phys. Lett.* **259** 313–20

[4] Niikura H, Lagara F, Hasbani R, Bandrauk A D, Ivanov M Yu, Villeneuve D M and Corkum P B 2002 Sub-laser-cycle electron pulses for probing molecular dynamics *Nature* **417** 917–22
[5] Niikura H, Lagara F, Hasbani R, Ivanov M Yu, Villeneuve D M and Corkum P B 2003 Probing molecular dynamics with attosecond resolution using correlated wave packet pairs *Nature* **421** 826–9
[6] Scrinzi A, Ivanov M Yu, Kienberger R and Villeneuve D M 2006 Attosecond physics *J. Phys. B: At. Mol. Opt. Phys.* **39** R1–R37
[7] Paulus G G, Becker W, Nicklich W and Walther H A 1994 Rescattering effects in above-threshold ionization: a classical-model *J. Phys. B: At. Mol. Opt. Phys.* **27** L703–8
[8] Hu S X and Collins L A 2004 Imaging molecular structures by electron diffraction using an intense few-cycle pulse *Phys. Rev. Lett.* **94** 073004
[9] Harvey A G and Tennsyon J 2007 Electron re-scattering from H_2 and CO_2 using *R*-matrix techniques *J. Mod. Opt.* **54** 1099–106
[10] Baker S, Robinson J S, Haworth C A, Teng H, Smith R A, Chirila C C, Lein M, Tisch J W G and Marangos J P 2006 Probing proton dynamics in molecules on an attosecond time scale *Science* **312** 424–7
[11] Mairesse Y, Levesque J, Dudovich N, Corkum P B and Villeneuve D M 2008 High harmonic generation from aligned molecules-amplitude and polarization *J. Mod. Opt.* **55** 2591–602
[12] Mairesse Y, Dudovich N, Levesque J, Ivanov M Yu, Corkum P B and Villeneuve D M 2008 Electron wavepacket control with elliptically polarized laser light in high harmonic generation from aligned molecules *New J. Phys.* **10** 025015
[13] Morgan L A, Tennyson J and Gillan C J 1998 The UK molecular *R*-matrix codes *Comput. Phys. Commun.* **114** 120–8
[14] Gorfinkiel J D and Tennyson J 2004 Electron-H_3^+ collisions at intermediate energies *J. Phys. B: At. Mol. Opt. Phys.* **37** L343–L350
[15] Colgan J, Pindzola M S, Robicheaux F, Kaiser C, Murray A J and Madison D H 2008 Differential cross sections for the ionization of oriented H_2 molecules by electron impact *Phys. Rev. Lett.* **101** 233201
[16] Burke P G and Berrington K A (ed) 1993 *Atomic and Molecular Processes, an R-matrix Approach* (Bristol: Institute of Physics Publishing)
[17] Morrison M A and Sun W 1995 *Computational Methods for Electron–Molecule Collisions* ed W M Hou and F A Gianturco (New York: Plenum) chapter 6, pp 184–5
[18] Brink D M and Satchler G R 1968 *Angular Momentum* (Oxford: Oxford University Press) chapter 2, pp 20–27
[19] Malegat L 1990 DCS—a program for calculating differential cross sections for the electronic excitation of diatomic molecules at fixed nuclei *Comput. Phys. Commun.* **60** 391–404
[20] Tashiro M, Morokuma K and Tennyson J 2006 *R*-matrix calculation of differential cross section for low-energy electron collisions with ground and electronically excited O_2 molecules *Phys. Rev.* A **74** 022706
[21] Tennyson J 1996 Resonance parameters and quantum defects for super-excited H_2 *At. Data Nucl. Data Tables* **64** 253–77
[22] Horsley J A and Fink W H 1969 Study of the electronic structure of the ions CO_2^+ and N_2O^+ by the LCAO-MO-SCF method *J. Phys. B: At. Mol. Phys.* **2** 1261–70
[23] Morgan L A, Gillan C J, Tennyson J and Chen X 1997 *R*-matrix calculations for polyatomic molecules: electron scattering by N_2O *J. Phys. B: At. Mol. Opt. Phys.* **30** 4087–96
[24] Graefe S and Ivanov M Yu 2008 On the electron localization dynamics induced by laser-driven electronic rescattering *J. Mod. Opt.* **55** 2557–72
[25] Tennyson J, Noble C J and Burke P G 1986 Continuum states of the hydrogen molecule with the *R*-matrix method *Int. J. Quantum Chem.* **29** 1033–42
[26] Burke P G and Burke V M 1997 Time-dependent *R*-matrix theory of multiphoton processes *J. Phys. B: At. Mol. Opt. Phys.* **30** L383–91
[27] van der Hart H W, Lysagt M A and Burke P G 2007 Time-dependent multielectron dynamics of Ar in intense short laser pulses *Phys. Rev.* A **76** 043405